Plasma Plume Characterization of Electric Solid Propellant Pulsed Microthrusters

Matthew S. Glascock,[1] and Joshua L. Rovey,[2]
Missouri University of Science and Technology, Rolla, Missouri, 65409

and

Shae Williams,[3] and Jason Thrasher,[4]
Digital Solid State Propulsion, Reno, Nevada, 89511

Electric Solid Propellants are an exciting potential option for propulsion because they are ignited only by an applied electric current. This leads to exciting capabilities such as on-demand throttling and re-ignition, and insensitivity to accidental ignition by spark, impact or open flame. Digital Solid State Propulsion has developed a pulsed microthruster using an electric solid propellant. In this work, the plasma plume created by these microthrusters is investigated using a nude Faraday Probe, an array of single Langmuir Probes, a triple Langmuir probe and Residual Gas Analysis. The thruster was tested at a vacuum level of 2×10^{-5} Torr. Results indicate a peak centerline ion current density of about 200 mA/cm^2, peak electron temperature of about 1 eV and peak electron density of between 1 and 2×10^{11} cm^{-3}. Additionally, ionization fraction estimates are < 1% of an ablation mass bit of about 250 μg on average. Exhaust velocity estimates are largely inconclusive, but are on the order of a few km/s.

Nomenclature

A_n	=	probe collection area of probe n; n = 1, 2, 3
L	=	length of exposed probe tip
D	=	diameter of exposed probe tip
P_n	=	probe label
V_n	=	voltage of probe n, with respect to space potential
V_p	=	space potential
V_f	=	floating potential, with respect to ground
V_{d2}	=	voltage difference between probe 1 and probe 2
V_{d3}	=	voltage difference between probe 1 and probe 3; bias voltage
I_n	=	current flow in probe n
$T_e(t)$	=	electron temperature
T_e^{mx}	=	max electron temperature
$n_e(t)$	=	electron number density
n_e^{mx}	=	max electron number density
n_i	=	ion number density
n_n	=	neutral particle number density
m_i	=	mass of ion species i
V_{ex}	=	exhaust velocity (of ions)

---

[1] Graduate Research Assistant, Aerospace Plasma Laboratory, Mechanical and Aerospace Engineering, 160 Toomey Hall, 400 W. 13th Street, Student Member AIAA.

[2] Associate Professor of Aerospace Engineering, Mechanical and Aerospace Engineering, 292D Toomey Hall, 400 W. 13th Street, AIAA Associate Fellow.

[3] Chief Engineer, Aerospace Engineering, 5475 Louie Lane Suite D, Full Member AIAA.

[4] Engineer, Aerospace Engineering, 5475 Louie Lane Suite D, Full Member AIAA.

I. Introduction

THE development of Electric Solid Propellants[1-5] (ESP's) is an emerging topic of research with major implications in the field of space propulsion from the micro to macro scale. ESP's offer new and exciting capabilities in the field of solid rocket propulsion, such as on-demand throttling and extinguishment/re-ignition. Additionally, some of these propellants, like the type being developed by the small business Digital Solid State Propulsion (DSSP) in Nevada, are insensitive to ignition by spark, impact or open flame, making them much safer to transport and handle. This higher performance electric propellant (HIPEP) is easily manufactured and uses "green" ingredients. Recently, DSSP has developed a microthruster utilizing this green electric solid propellant that operates in a mode very similar to a traditional type of electric propulsion, the coaxial Pulsed Plasma Thruster (PPT). These microthrusters are extremely well suited to widespread small spacecraft applications due to a very small size (1/8" diameter, 1" length), low power requirements (2-5 W capacitor charging cycle) and ease of handling and integration. Because these thrusters are new to the community, a focus has been on characterizing all aspects of the thruster performance and plasma characteristics in order to effectively compare these thrusters to the technologies already available in the electric propulsion field.

The Pulsed Plasma Thruster (PPT) is a type of in-space electric propulsion system studied extensively in the literature[6] and flown successfully on spacecraft in past years. The PPT, a type of magnetoplasmadynamic device[7], operates by pulsing a high-current discharge between electrodes across the exposed surface of a solid insulating propellant, typically Teflon. This arc ablates a sheet of the propellant from the surface and vaporizes, ionizes and heats the propellant sheet. The plasma sheet is then accelerated to very high exit velocities (up to 50 km/s) by the electromagnetic body force resulting from the magnetic field present in the PPT channel. Electrothermal processes are also typically a major contributor to the high exhaust velocities due to the inherently high temperatures associated with the PPT plasma sheet created by the arc discharge. These thrusters are primarily used for stationkeeping needs[8-11], but their performance can be extended to use for orbit transfers[12], formation flying[13] and attitude control[14,15].

II. Thruster Design

Digital Solid State Propulsion (DSSP) has developed solid electric propellants for use in space propulsion systems from the micro to the macro scale. One of DSSP's many innovations is the **Hi**gh **P**erformance **E**lectric **P**ropellant[5] (HIPEP), a hydroxyl ammonium nitrate (HAN) based solution solid manufactured using benign processes and "green" ingredients, mixed in standard chemical glassware and cured conveniently at room temperatures (35°C/95°F). Relatively safe to handle and classified under DOT as a 1.4S explosive, the HIPEP is much more convenient to transport and work with than conventional solid rocket propellants. The relatively high standard specific impulse (Isp) of the HIPEP, combined with the simple manufacturing processes and the nano-scale uniformity of the cured propellant makes the HIPEP well suited to microthruster (small-sat) applications. Shortly after developing the HIPEP, DSSP developed a co-axial microthruster ideal for integration on a small spacecraft[16]. The HIPEP microthruster, described in Figure 1 below, operates in a method quite similar to traditional pulsed plasma thrusters. The HIPEP is cured in the space between an outer electrode tube (1/8" diameter, ~1" long) and an inner electrode rod (3/64" diameter) coated with insulation. By applying a relatively low voltage, 300 V, discharge from a capacitor bank for a short duration pulse, about 1 ms, a thin annular sheet of the HIPEP is ablated and expelled from the thruster.
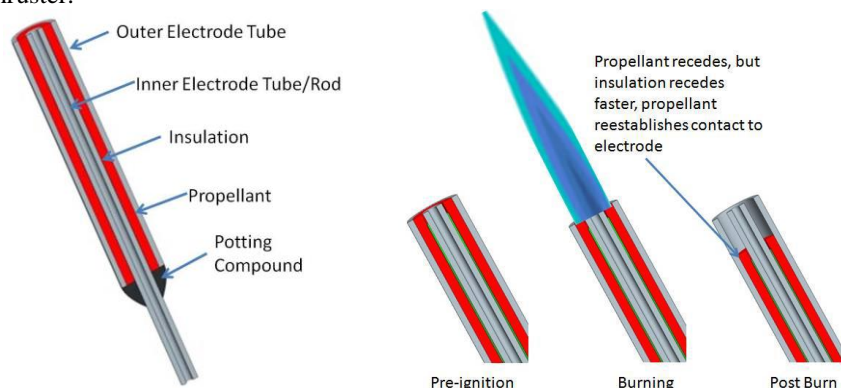

Figure 1: CAD Model illustrating composition and operation of the HIPEP microthruster. Current passing through the propellant ablates it and the insulation on the center electrode rod. Adapted from reference[5].

American Institute of Aeronautics and Astronautics

The small size and low power requirement of this microthruster lends itself greatly to application as a small spacecraft propulsion system. Requirements for a small spacecraft would be minimal, given that there is no need for a propellant tank (i.e. no large volume or high pressure requirement) and the power processing unit would have minimal design requirements given the lower power (< 5 W) applied to charge the capacitor bank. While operation of the HIPEP thruster is similar to a traditional PPT operation, there are some key differences. Teflon is a fluorocarbon solid, while HIPEP is a soft-solid mixture of HAN oxidizer (an inorganic ionic liquid) and polyvinyl alcohol (PVA) fuel binder, which make up 95% of the propellant, as shown in Table I. In a typical PPT, the Teflon is an electrical insulator between the electrodes; HIPEP has a high electrical conductivity. This is suspected to be a main difference in the fundamental operation of the thruster. The pulsed electric current is actually being conducted through the HIPEP propellant in the microthruster; in a PPT an arc is passed over the surface of the solid Teflon. Additionally, in a traditional PPT, the propellant is fed into the thruster whereas the propellant is burned up in the HIPEP microthruster, leading to changing operating conditions over the lifetime of the thruster. It is currently unclear how these different propellant properties lead to differences in operation and performance in a PPT.

Table I. Chemical make-up of the High Performance Electric Propellant tested in the microthrusters.

Chemical Name	Chemical Formula	Percentage (by mass)	Molecular Mass (g/mol)
Hydroxyl Ammonium Nitrate (HAN)	$H_4N_2O_4$	75%	96
Polyvinyl Alcohol (PVA)	C_2H_4O	20%	44
Ammonium Nitrate (AN)	NH_4NO_3	5%	80

III. Diagnostic Apparatus

Characterization of the plasma plume created during a pulse is generally the first step of analyzing a PPT system, and the primary focus of this work. Plume velocity distribution, plasma density and temperature, and current density are very useful in analyzing performance of a PPT. Work on plasma plume characterization of the microthruster has been conducted at Missouri S&T, who has partnered with DSSP to analyze the microthruster. A number of prevalent PPT plume diagnostics were prepared and used for the analysis of the microthruster. Faraday probe[17,18] measurements for bulk plasma current, an array of single Langmuir probes[19,20] for spatial plume current and velocity and a Langmuir triple probe[21-23] to determine plasma densities and temperatures were employed.

A. Faraday Probe

The nude Faraday Probe (FP) is used to measure the ion current density in the plume of an electric propulsion device, be it an electrostatic device such as a Hall Effect thruster[18], or a pulsed device such as the PPT. Of course, the nude Faraday probe has a number of shortcomings, most notably of which is a sensitivity to vacuum facility effects and elevated backpressures[24]. However, this probe will allow a rough first look at the ion current density and plume velocity of an uncharacterized device. The Faraday probe used in this work, pictured in Figure 2 at right, is fairly simple in design; both the center collector plate and the outer shell are conductors and are biased to the same nominal voltage by separate supplies. The probe is biased to a negative voltage (in this work, -30 V relative to ground) to repel

Figure 2. Faraday Probe integrated into large vacuum chamber diagnostic probe arm.

American Institute of Aeronautics and Astronautics

stray electrons and encourage the collection of ions. The center collector is then connected to a measurement circuit similar to that of a traditional planar Langmuir probe. Monitoring the current draw through the collector of the Faraday probe provides a rough ion current density of the plume. The collector is about 2.54 cm (1") in diameter, giving it a circular (planar) collection area of about 5 cm^2. Because the size of this probe is quite large relative to the microthruster and the estimated size of the plasma plume created, it is assumed that the probe will collect a large majority of the ions present in the plume when positioned near (~5 cm) the thruster exhaust and aligned with the axis of the microthruster. Near-field Faraday probe results can be used to estimate the ionization fraction of the plasma plume and will also allow for ion exhaust velocity measurements. Additionally, the Faraday probe was integrated onto mobile translation stages in the vacuum test facility, allowing it to make measurements of the ion current density at various centerline and off-centerline locations.

B. Langmuir Probe Array

Langmuir probe diagnostics are fairly well outlined and widely used in the study of plasmas[20]. In this work, an array of five independently biased and measured single Langmuir probes with a collection area of ~0.625 cm (Figure 3a) are used to resolve a spatial distribution of ion current in the microthruster plume. Each probe is approximately 2.5 cm long and 0.25 cm in diameter, giving each an L/D value of 10. The probes are arrayed in a flat plane normal to the thruster axis that can translate along the axis of the thruster. Making measurements at a number of predetermined axial locations for the array, shown in Figure 3b, allows the shape and "size" of the plume to be determined. Additionally, this will allow for acquiring a spatial distribution of ion current collected. The spatial ion current distribution provides refined estimates of ionization fraction of the plasma plume, among other conclusions.
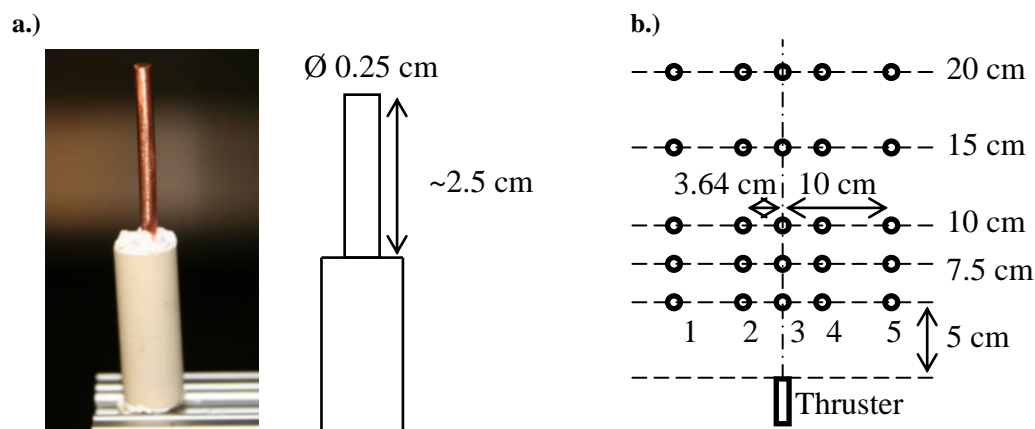
a.)   b.)

Figure 3. a.) Single Langmuir probe used for array diagnostics and b.) probe array frame dimensions and locations relative to microthruster.

C. Langmuir Triple Probe

The final diagnostic used in this work is the Langmuir Triple Probe (LTP). This is a common, sophisticated tool used in the study of plasmas that offers a more versatile operation method over the single Langmuir probe. Using the traditional method of triple Langmuir probe diagnostic theory, electron density and electron temperature measurements can be made at various locations in the plume as a function of time. Recent efforts have shown that the triple probe is well suited to operation in pulsed environments, and can be very informative in the diagnostic process of a conventional pulsed plasma thruster[21-23]. Additionally, the triple probe has the potential to verify (or debunk) the measurements of exhaust velocity made using the previously outlined diagnostic techniques. The physical design of the triple probe is uncomplicated. As shown in Figure 4a below, the main body of the probe is a nonconductive, quad-bore alumina tube. Long pieces of ~0.5 mm dia. tungsten wire are inserted into three of these bores, creating the three isolated probe tips of ~5 mm in length; the remaining bore is plugged with a ceramic adhesive. On the other end of the probe, the tungsten wires connect to a individual stamdard RF cables inside a grounded enclosure to ensure the connections are well shielded.
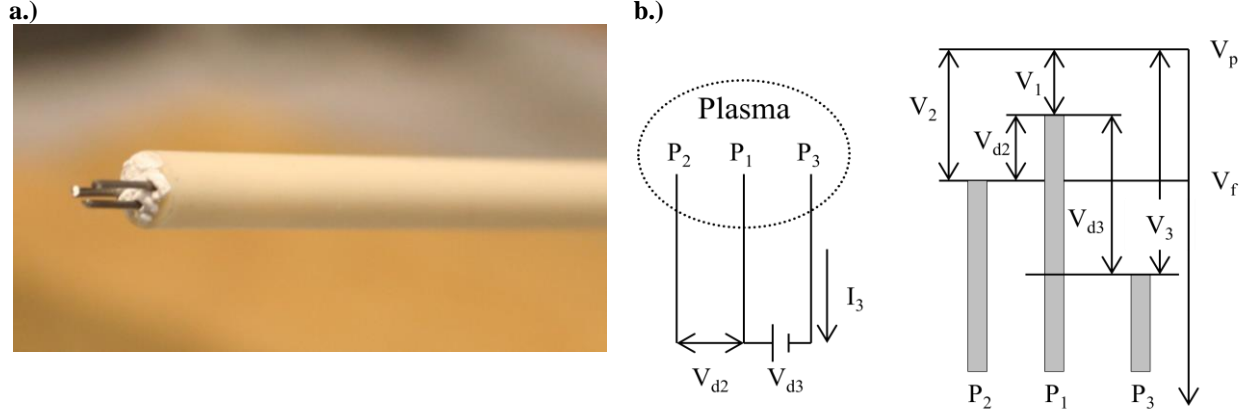
American Institute of Aeronautics and Astronautics

Figure 4: Langmuir Triple Probe a.) physical design and b.) electrical setup.

In this work, the triple probe was operated in what is referred to as "voltage-mode," wherein (as in Figure 4 above) three identical probes are inserted into the plasma. All three probes are floating with respect to ground (V_f), and a bias voltage difference, V_{d3}, is applied externally to two of the probes via a battery. In this work, V_{d3} was selected as a nominal 27 V, supplied via three 9V batteries in series. During a pulse, the voltage difference V_{d2} is measured viaa differential voltage probe and the probe current, I_3, is measured via a current monitor. The high voltage differential probe was selected because these probes were found to be less susceptible to signal noise than digitally subtracting signals on an oscilloscope, or using differential operational amplifiers[22]. These measurements are displayed as a function of time during testing on a 4-channel Tektronix DPO2000 series oscilloscope. Through the Langmuir Triple Probe theory from Chen and Sekiguchi[25], outlined below, these measurements $V_{d2}(t)$ and $I_3(t)$ can be used to directly calculate the plasma electron temperature, $T_e(t)$, and the plasma density, $n_e(t)$ via equations (1) and (2) below.

$$\frac{1 - \exp\left(-\frac{V_{d2}}{T_e}\right)}{1 - \exp\left(-\frac{V_{d3}}{T_e}\right)} = \frac{1}{2} \tag{1}$$

$$n_e = \frac{m_i^{\frac{1}{2}}\left(\frac{I_3}{A_3}\right)1.05 \times 10^9}{(T_e)^{\frac{1}{2}}\left(\exp\left(\frac{V_{d2}}{T_e}\right) - 1\right)} \tag{2}$$

Where T_e is the electron temperature of the plasma in eV, m_i is the plasma species (assumed) mass number, I_3 the measured probe current in μA, A_3 the individual probe collection area in mm^2 and n_e is the plasma density measured in cm^{-3}. In the equations above, the applied voltage difference V_{d3} is assumed constant during each pulse; testing found that the current draw on the batteries supplying this voltage was negligible and thus a valid assumption. Additionally, the density equation requires a plasma species mass. In this work, this was taken as the mass number of atomic carbon (C_{12}) in order to develop a rough estimate of the density of plasma species relative to singly ionized carbon atoms, which may in fact make up a large part of the actual plume.

D. Auxiliary Diagnostics

Apart from the above outlined plasma diagnostics, a few other key properties of the microthruster were investigated, including residual gas analysis (RGA) of the plume and the average mass expelled on each pulse, called the mass bit. RGA results are very beneficial when estimating the ionization fraction of the microthruster, as it will allow a better estimate of exhaust gas species. The residual gas analyzer used for this work was an Extorr XT100 model, a quadrupole RGA with included Pirani gauge and hot cathode ion gauge. This model's resolution is adjustable based on the selected mass range (max width 1-100 amu), but is greater than 0.5 amu at 10% peak height; the sensitivity is 5×10^{-4} A/Torr into the detector and the device has a minimum detectable partial pressure of 10^{-11} Torr. The microthruster was tested primarily in the large (6' dia., 10' lg.) space and high altitude vacuum facility at Missouri S&T, which has a nominal base pressure of 2×10^{-5} Torr while operating with 2 of 4 oil vapor diffusion

pumps active. Additionally, the mass bit expelled per pulse is a quality of interest in the testing of the microthrusters. In order to estimate this, the mass of a microthruster is measured immediately prior to testing and again immediately following testing. The mass scale used has a resolution of 1 mg, with some noise on the order of that resolution. With careful tabulation of the number of pulses logged on a microthruster during testing, a rough estimate ($\pm$5%) of the average mass expelled per pulse (the mass bit) value can be determined. This number can then be used to estimate the total number of particles (ionized and neutral) present in the plume during a pulse. Combining this with the above plasma diagnostics and gas species analysis provides a refined estimate of the fraction of ionized particles to neutrals in the microthruster plume.

IV. Experimental Results

Due to the pulsed nature of the microthrusters, data from a single microthruster can include time-resolved data for many (150+) pulses. As such, the results presented in this section are either data that are meant to be representative of the generally observed results, or data that is averaged over a number of pulses from a single thruster, where applicable.

A. Faraday Probe Results

a.)   b.)
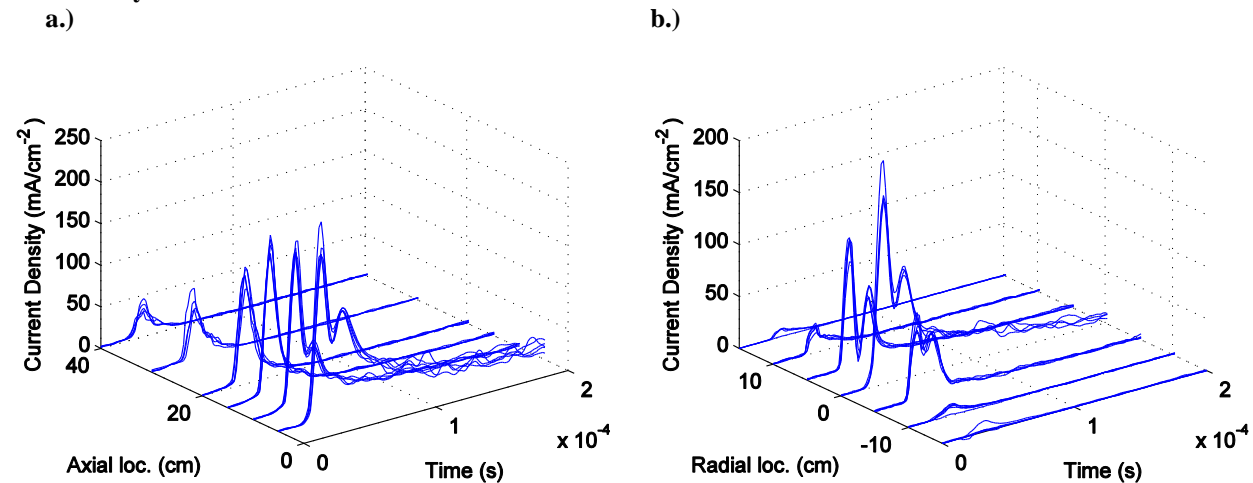

Figure 5. Ion current density as measured by the nude Faraday probe at locations a.) 5, 10, 15, 20, 30 and 40 cm downstream on the thruster centerline and b.) $\pm$5, 10 and 15 cm off-centerline at 5 cm downstream.

Figure 5 above shows 5 samples per location of the ion current density as a function of time as measured by the nude Faraday probe at the 5, 10, 15, 20, 30 and 40 cm downstream locations along the centerline of the thruster. The greatest ion current density is at the 5 cm location, closest to the thruster nozzle, which peaks at about 230 mA/cm^2 on average. Moving further from the thruster nozzle, the ion current density decreases by only about 15% (~190 mA/cm^2) at the 10 and 15 cm locations, but quickly decreases further downstream to about 60% of that peak at 20 cm. Further, the far-field ion current measurement at 40 cm downstream is only about 20% of that peak value (~50 mA/cm^2). Also note how the shape of the measurement pulse has two distinct peaks at the locations near the thruster. Moving further downstream, the second peak shifts to a later time as well as decreases in magnitude relative to the first peak. At the 5 cm location, the second peak occurs ~18 μs later than the primary peak, and is about one-half the magnitude. Comparably, at the 10 cm location, the second peak occurs ~24 μs later and is about one-third the magnitude of the primary peak. Beyond these locations, the secondary peak becomes difficult to discern from noise due to a very small magnitude. In Figure 5b, a similar graph shows the ion current density measurements at 5, 10 and 15 cm locations in the radial, or off-centerline, direction at 5 cm downstream. These measurements show a similar trend with the greatest ion density on the centerline location with a peak of ~200 mA/cm^2. However the ion current density falls off more rapidly with the radial distance from centerline, decreasing by 45-55% at 5 cm off-centerline and by more than an order of magnitude (~15 mA/cm^2) at 10 cm off centerline. Further, the ion current density measured at the 15 cm off-centerline locations are nearly negligible compared to the peak, at about 1 or 2 mA/cm^2.

American Institute of Aeronautics and Astronautics

Figure 6 below shows the profile of total charge collected in Coulombs for both a centerline distribution as well as off-centerline distributions. This result is obtained, of course by integrating each set of current measurement data shown in Figure 5 above, first for the 5, 10, 15, 20, 30 and 40 cm downstream on-centerline locations and then for the 5, 10 and 15 cm locations off-centerline. A familiar trend is observed along centerline (Figure 6a), where the peak measurement of collected charge is ~4×10^{-5} C at the 5 cm location, and that value rapidly decreases with distance downstream to 50% of that peak at 10 cm, 20% at 20 cm and more than an order of magnitude lower at the 40 cm location, where the collected charge measurement is ~4×10^{-6} C. Similarly, the results from the off-centerline Faraday Probe testing in Figure 6b show a peak value of ~3.5×10^{-5} C at the centerline location that decreases by 75% at 5 cm in the radial direction, more than an order of magnitude at 10 cm (1.6 μC), and becomes negligible (< 0.1 μC) relative to the peak at 15 cm or more off-centerline. FP results were quite consistent across the samples taken of 100-150 pulses on three separate microthrusters, with a standard deviation in peak ion current density of just under 40 mA/cm^2 on centerline at 5 cm downstream, and decreasing to less than 10 mA/cm^2 at locations further downstream and off-centerline. Variance in the peak charge collection is wider, due to an added variance in the pulse duration, coming in at about $\pm$30% of the mean, ~3.5×10^{-5} Coulombs. Standard deviation of this measurement also decreases with increased downstream and off-centerline to a minimum of about 0.2 Coulombs. Due to low noise and minimized edge effects in the Faraday probe, measurement error is estimated to be < 10%.
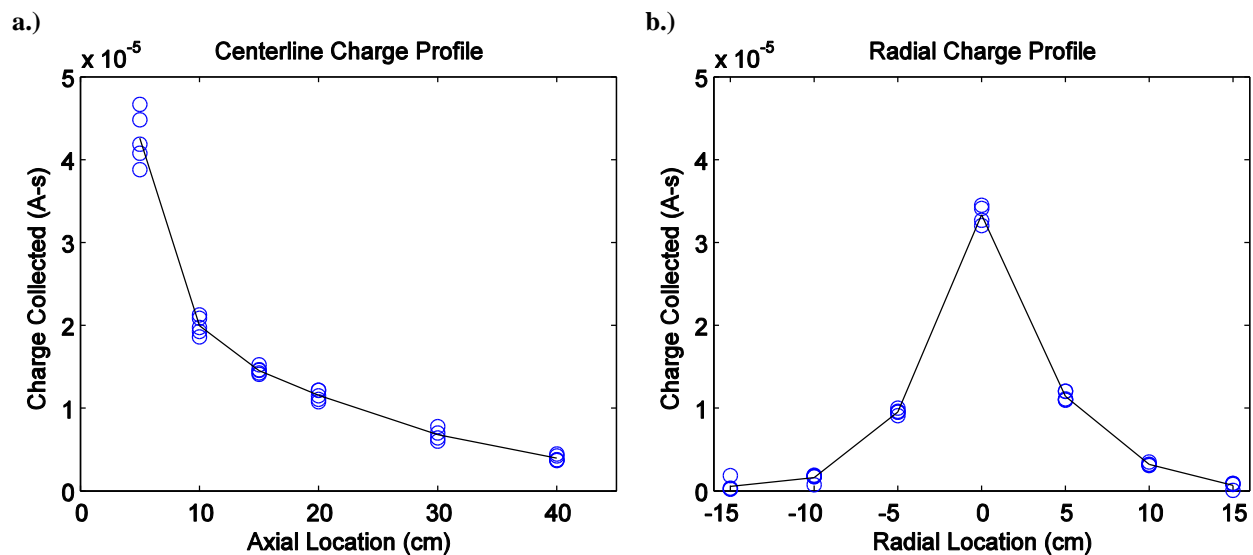
a.) b.)

Figure 6. Integrated Faraday Probe results indicating total ion charge collected in Coulombs for a few samples and the trendline (average) for the a.) centerline locations and b.) off-centerline locations.

B. Probe Array Results

Ion current density measurements can be obtained from the single Langmuir probe array were expected in a similar method to that of the nude Faraday probe. Integrating those measurements in time provides a measurement of the total ion charge collected at each location of the probes in the array. Figure 7 below illustrates the spatial map of the ion charge distribution in the plasma plume of the microthruster. As detailed in the Section III-B above, the Langmuir probe array results are shown for the 0, $\pm$3.64 and $\pm$10 cm locations off-centerline for a given location downstream. The probe array was positioned at 5, 7.5, 10, 15 and 20 cm locations downstream of the thruster, creating a 25 node (5$\times$5) spatial mesh of ion charge measurements. The peak ion charge value of about 1.4×10^{-6} C was measured at the 5 cm axial, 0 cm radial location. The trend observed along centerline is familiar; the ion charge collected decreases by about 20% at 7.5 cm, 50% at 10 cm, 70% at 15 cm and by almost 80% (3.2×10^{-7} C) at the 20 cm downstream location. In the off-centerline direction, however, a new trend is observed. The ion charge collection measurement at the 5 cm downstream location falls off to ~2×10^{-7} C in the positive radial direction, but only to ~2×10^{-7} C in the negative direction off-centerline. This asymmetric trend in the off-centerline measurements is observed at all of the downstream array locations. The spatial map thus indicates a characteristic asymmetric appearance to the ion charge distribution of the thruster plume. More details and discussion on this result are to follow in Section V below.
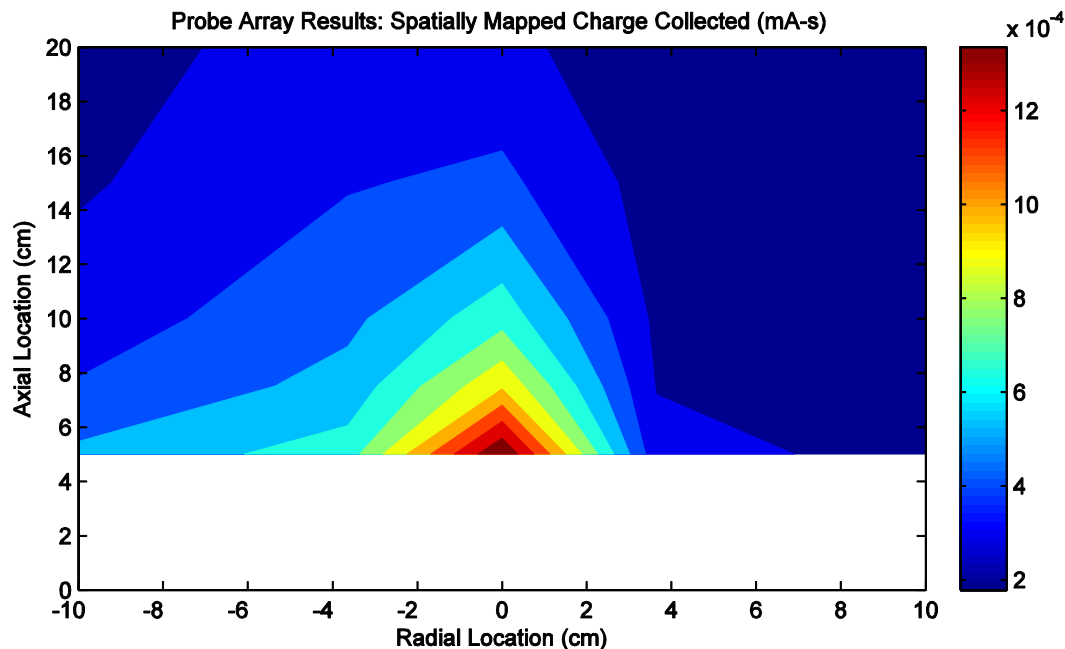
American Institute of Aeronautics and Astronautics

Figure 7. Spatial map of total charge collected as measured by the single Langmuir probe array.

C. Langmuir Triple Probe Results

The triple Langmuir probe provides measurements of electron temperature (T_e) and density (n_e) as a function of time for each pulse of a microthruster. Typical results from the triple probe show a peak electron temperature of a single digit eV and a peak electron density on the order of 10^{11} cm^{-3}. In the results most (> 95%) of the pulses measured, these peaks occur simultaneously, at least within the 1 μs resolution of the oscilloscope. Figure 8 below shows the trends of peak electron temperature and density for the lifetime of a microthruster. These trends show a variance of up to 200% or more in both the peak electron temperature and density for the first ~50-60 pulses. After that, the triple probe results indicate an average peak electron temperature of about 1 eV, which agrees with the ion current density results when compared to the mass bit data. Additionally, the triple probe results indicate an average peak of about 1.5×10^{11}, four or more orders of magnitude lower than a typical Teflon PPT[6,22]. Further discussion of these trends, along with the ionization fraction and the exhaust velocity of the plume is detailed in Section V below. Triple probe results were excessively noisy and variable, and the estimated error in measurement is about 40%. Additionally, the low density measurements may indicate an invalid thin sheath assumption in LTP theory.
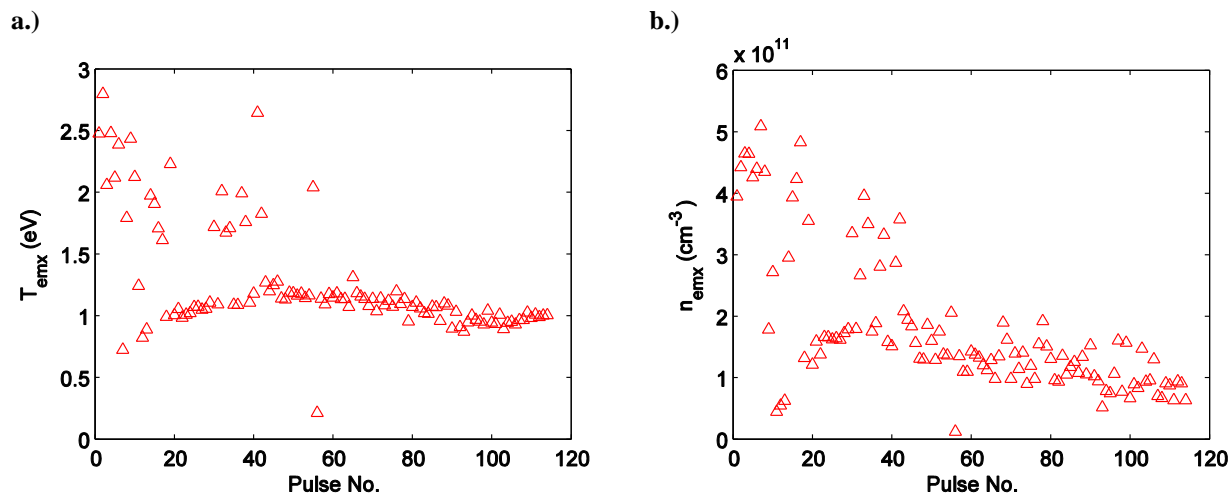
a.)

b.)

Figure 8: Langmuir Triple Probe result trends for a.) peak electron temperature and b.) peak electron density for the lifetime of a single microthruster.

8

American Institute of Aeronautics and Astronautics

D. RGA Results

Residual Gas Analysis (RGA) of the plume allows for estimation of the gas species present in the exhaust mixture of the microthruster. However, due to the slow operation of the RGA system, it is hard to capture an accurate representation of all the gas species for each pulse, as many of the species are present in such low concentrations and for very short times, the RGA simply will not detect them. Figure 9 below is a representative sample of RGA data from a single pulse. RGA data samples similar to that shown in Figure 9 were taken for 40 pulses of a single microthruster, 20 pulses in the early lifetime (1-20), and 20 pulses in the later lifetime (50-70). Note that the time scale here is irrelevant as the data recording is started manually a short time before thruster pulse in order to capture the entire pulse and a significantly large sample of time afterward. The pulse occurred at around 3 seconds in Figure 9, which shows a marked increase in diatomic nitrogen, hydrogen and oxygen, water vapor and carbon dioxide of a few percent of that species background partial pressure. The small increase in each species is on the time scale of one or two seconds, which is about 10^3 times longer than the time length of the microthruster pulse, typically 1 ms.
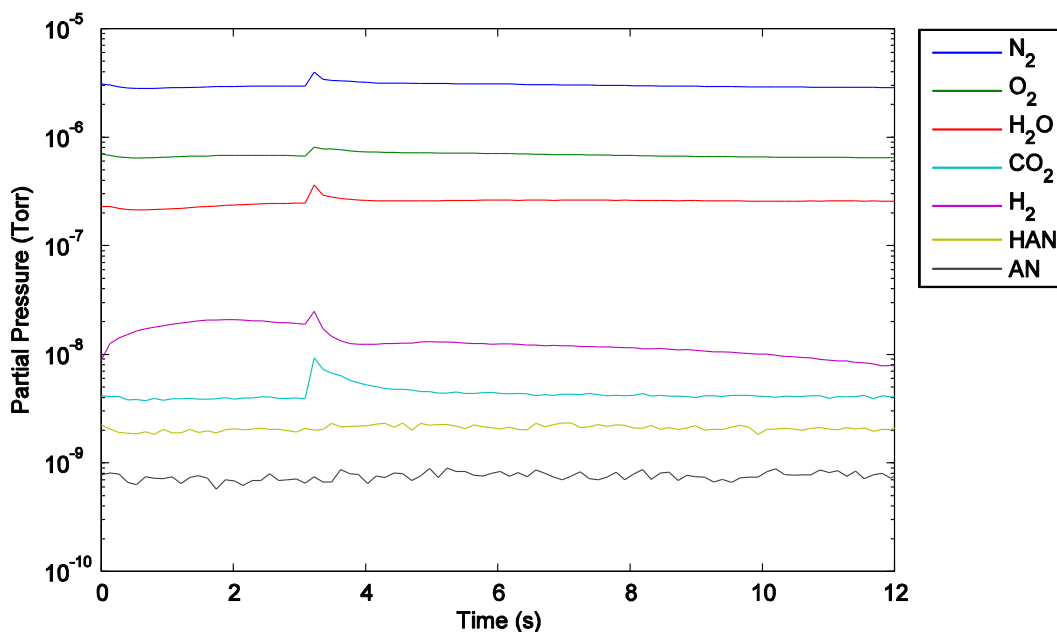

Figure 9: Residual Gas Analysis data from a single pulse of the HIPEP microthruster representative of results common for most of the data acquired.

Not shown on this particular sample is the data for diatomic Carbon (C_2), as it was a particularly noisy and negligible (10^{-12} Torr) measurement in this particular sample; however, it was observed in a number of other samples. Additionally, this sample shows no obvious increase in the partial pressure of either hydroxyl ammonium nitrate (HAN) or ammonium nitrate (AN), two of the primary constituents of the HIPEP. However, this is not a universal trend; in fact, over 25% of the RGA data samples taken from the microthruster show an brief increase in the partial pressure of HAN, AN, or both for a shorter period of time (< 1 s) than the molecules seen above. This is likely an artifact of the RGA's slow operation, and may indicate that either compound is actually being expelled in most (or all) pulses, but that the RGA is unable to consistently detect the small amounts of HAN or AN present for such a short time in the plume. The same is true of some of the intermediate combustion products of the propellant, such as nitric acid (NO_3), nitric oxide (NO), and NO_2. RGA testing on a separate microthruster and date show evidence of these nitrogen oxide intermediate compounds for short (< 1s) durations, much like was observed with the HAN and AN. Of course, the fairly consistent detection of the expected plume constituents (N_2, CO_2, H_2O, C_2) is an indicator that the plume is also largely made up of the expected products of full combustion. For instance, small ($5 - 20\%$) increases in the partial pressure of N2 were observed in nearly every pulse (35 of 40) sampled for the microthruster. Larger increases of partial pressure by 100% or more over the background for H2O and CO2 were observed in about 10% of the samples, especially in the early pulse lifetime of the thruster (pulse $1 - 20$). In the later pulses (pulse $50 - 70$), C2 was observed in 18 of the 20 pulses sampled, at partial pressure increases commonly $20 - 50\%$, but 120% or more in some cases.

American Institute of Aeronautics and Astronautics

V. Discussion and Analysis

A. Ion Current Density

One observation made in the Faraday Probe results is the dual peak nature of the current density measurements. This could be a result of a dual-wave type of plume often observed in pulsed plasma thrusters where one portion of the atoms in the plume are accelerated electromagnetically and the rest are accelerated thermally[30]. The thermally accelerated atoms do not travel as quickly as the other atoms/ions and thus are detected later. Potentially, this double peak measurement could also be a result of an observed "two-phase" discharge nature of the capacitors used to pulse the microthruster. The Faraday Probe also indicates a relatively low current density (>200 mA/cm^2) and charge collected (3.5×10^{-5} C) on centerline when compared to similar measurements on a typical PPT[17,31].

Referring back to Figure 7, the single probe array indicates an asymmetric current density profile. Potentially, this is because of the way the probe array was integrated in the test facility. There was an exposed portion of the conductive probe arm structure on the right-hand side (here, positive radial location) of the probe array setup when integrated. This may have interfered with ion collection, despite the majority of the structure being covered in a dielectric material, though further testing was unable to verify this theory. Because of this asymmetry, as well as considerable noise, the measurement error estimate is ~35%. Additionally, the probe array measures a much lower charge collection (~1×10^{-6} C) than the Faraday probe results. This is likely due to the presence of the multiple probes, and of course the small collection area (0.625 cm^2) of the probes compared to the Faraday Probe (5 cm^2).

B. Exhaust Species

The composition of the solid HIPEP is well understood (Table I), as well as the product species of *full* combustion/decomposition of the propellant[5]. However, due to the very short pulse and resident times in the operation of the microthruster, it is unlikely that full combustion of the propellant is achieved in every pulse. To characterize the exhaust species of the HIPEP, the RGA data like that in Figure 9 was utilized. For a given pulse, the increase in partial pressure for each species is compared to the increase in total pressure (i.e. the sum of all the increases in partial pressures) to determine the fraction of species present (or rather, detected) in that pulse. Extending this method to the 40 pulse sample of the thruster and averaging the results gives an average makeup by percent, based on the increase in partial pressure. Combining this information with the molecular weight of each species provides an accurate estimate of the *actual* gas species present in the exhaust plume of the thruster. Figure 10 below presents these estimates compared with the product species predicted from full combustion of the HIPEP. Unfortunately, RGA testing was only able to be conducted for a small sample of pulses from a single microthruster. In order to get a highly accurate estimate of the exhaust species, a larger number of samples (100+) from many microthrusters to get a solid baseline of exhaust species expelled on average.
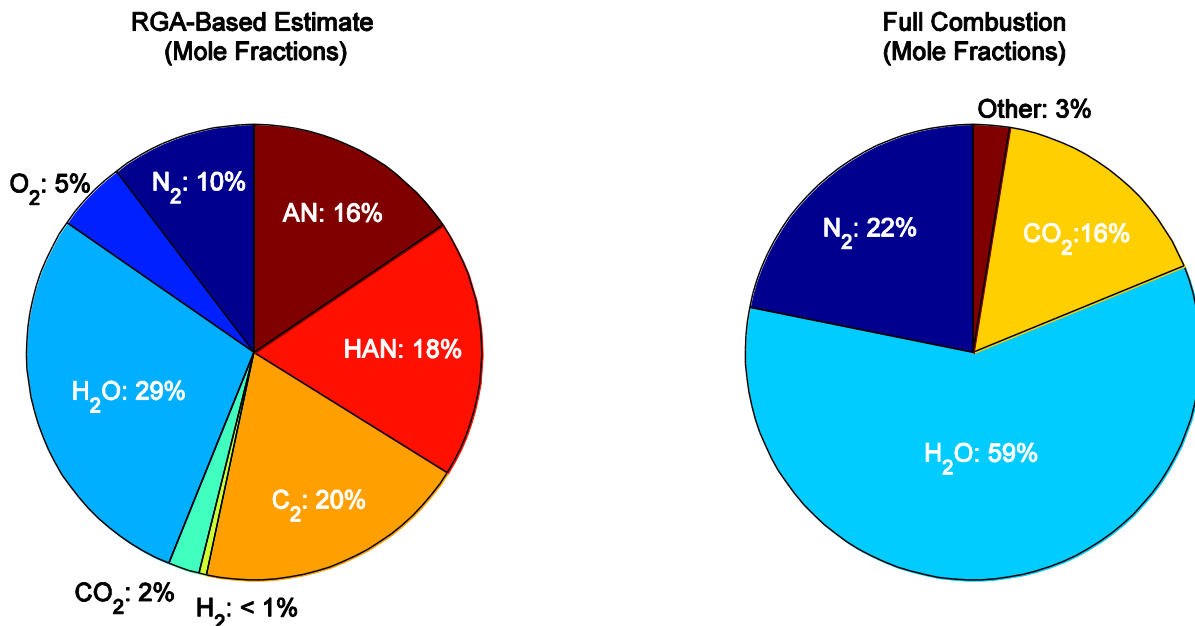

Figure 10. Plume exhaust gas species comparison based on RGA data and full combustion predictions.

10

American Institute of Aeronautics and Astronautics

C. Ionization Fraction

Of much interest in the characterization of these microthrusters is the fraction of total atoms and molecules present in the plume that have been ionized due to the pulsed discharge. In order to get a good estimate of this "ionization fraction," an understanding of the gas species present in the plume (both bulk and charged species) is required. Combining the above plume species formulation with the total charge collected data from both the Faraday Probe and Probe Array (compared in Figure 11 below), an estimate for ionization fraction can be obtained. Note the rather large discrepancy between the radial charge density measurements of the Faraday probe versus the Probe Array results. The peak probe array value (on centerline) is about 50% of the peak Faraday probe measurement. Most likely, the Faraday probe measurements are higher than realistic, as the probe is large and negatively biased, causing it to pick up the bulk of the plume at each location. On the other hand, the probe array provides simultaneous point measurements across the radial profile of the thruster plume, while being less sensitive to edge effects and stray charge-exchange ions than the nude Faraday Probe[18]. For this reason, it is suspected that the probe array results are closer to the actual charge density of the plume.
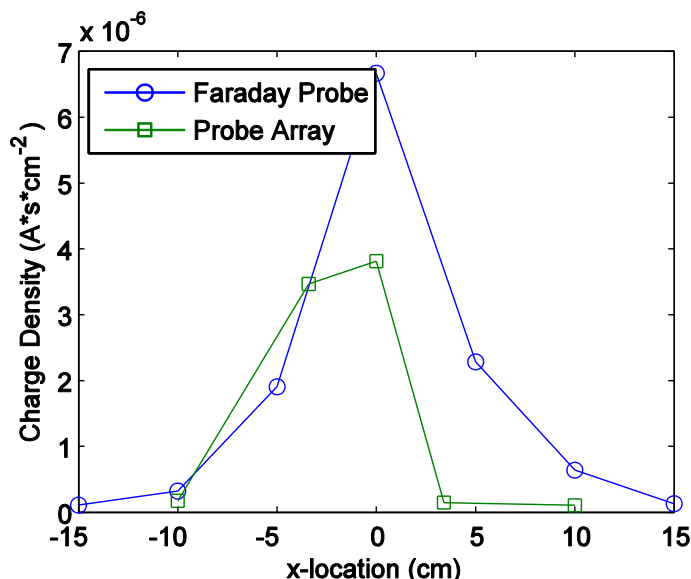

Figure 11. Comparison of charge density results of radial charge profile for Faraday probe and the array.

Revolving and integrating each of these data sets provides an estimate of the total charge carriers emitted in the cone of a single pulse of the thruster, assuming that all the charge carriers are singly ionized. As discussed in Section III-D, the mass ablated with each pulse, the mass bit, was determined experimentally by measuring the mass of a microthruster before and after testing. This method provided an average mass bit of about 250 µg drawn from 10 microthrusters at 100 or more pulses each. Combining this value and the exhaust gas species estimates yields the number of neutral particles present in the plume. The ionization fraction is then the fraction of singly ionized particles out of total particles. The final results are presented in Table II below. Note that the highlighted estimate (Probe Array charge density results, RGA estimate) is considered the most accurate physical estimate of the models compared here, though there is minimal difference between the results. These results are not typical for a traditional PPT, which usually exhibit plume ionization fractions of 10 – 20% of a 10 – 100 µg ablation mass[6].

Table II. Plasma plume ionization fraction (charge carriers to total particles) estimates.

Diagnostic	Exhaust Species Model	Number of Total Particles	Number of Charge Carriers	Ionization Fraction
Faraday Probe	Full Comb.	5.9217E+18	1.1119E+16	0.18777%
Faraday Probe	RGA Estimate	5.1260E+18	1.1119E+16	0.21692%
Probe Array	Full Comb.	5.9217E+18	5.6534E+14	0.00955%
Probe Array	RGA Estimate	5.1260E+18	5.6534E+14	0.01103%

11

American Institute of Aeronautics and Astronautics

D. Exhaust Velocity

In addition to the commonly examined ion plume characteristics, a measurement of ion exhaust velocity is important in the study of the microthrusters, as this measure will allow for an estimate of the specific impulse of the thruster to compare against specific impulse estimates drawn from micro thrust testing off-site. Two of the plasma diagnostics, the Faraday Probe and the Langmuir Triple Probe, were used to estimate the exhaust velocity. The fire event occurs when the current measurement through the thruster ignition circuit becomes positive, which is also when the oscilloscope triggers. From there, the time of the peak in current measured by the probe (Faraday or LTP) is compared to the time of the fire event to calculate a time of flight. When combined with the downstream location of the probe, an estimate of the plume velocity can be made. Initial Faraday probe results indicated an exhaust velocity of around 7000 km/s, but these results were unable to be replicated in further testing. Figure 12 below shows a comparison of the velocity estimates between the Faraday Probe and the preliminary Langmuir Triple Probe results. For all of the data in Figure 12, the downstream distance of the probe was nominally 5 cm. Calculated flight times range from 20 to 100 μs, which result in an exhaust velocity variance of +200% to -50%, especially in the first 50-60 samples of the triple probe data. Bit resolution of the data collection results in some artifacts in the early pulse data for the Faraday Probe data and the later pulse data for the triple probe data. However, after about 60 pulses into the thruster lifetime, the estimate is about 1 km/s on average. This velocity is lower than the predicted exhaust velocity based on the specific impulse values obtained from thrust testing conducted by the thruster manufacturer, DSSP. However, this value is on the order of typical mass-average PPT plume velocities (3-5 km/s), but much slower than typical ion velocities observed in Teflon PPT's, which are 10-50 km/s[6]. The excessive noise in the preliminary triple probe data yields an inconclusive estimate of exhaust velocity, and it is not yet understood what is causing this inconsistency.
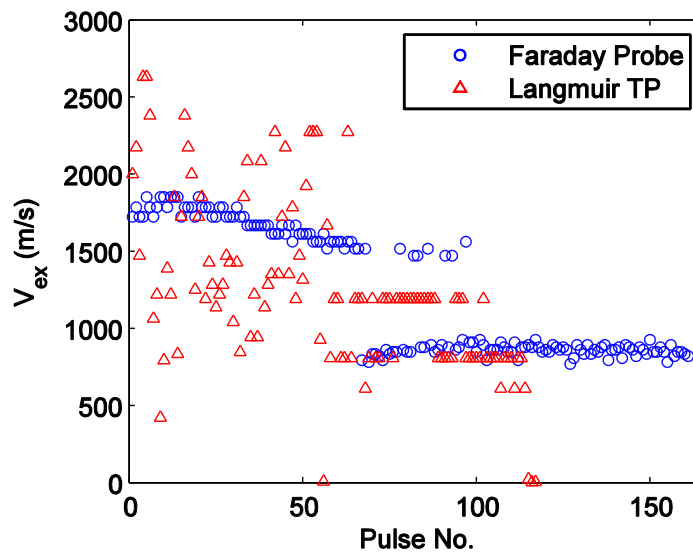

Figure 12: Ion/electron exhaust velocity as measured by the Faraday probe and Langmuir triple probe.

VI.   Conclusion

This experimental characterization of the plasma plume of a solid electric propellant microthruster was conducted with the goal of understanding the physics of the novel propellant, HIPEP, and the performance of the microthruster as a pulsed plasma thruster device. In understanding the plume of the device, further analysis of the applications and operation of the device in the hopes of developing a mature propulsion technology for small spacecraft. The diagnostics employed included a nude Faraday probe, an array of single Langmuir probes, a triple Langmuir probe and a residual gas analyzer. Centerline ion current density measurements were made at 5, 7.5, 10, 15, 20, 30 and 40 cm downstream location, and 5, 10 and 15 cm off-centerline in both directions. The peak ion current density measured was about 200 mA/cm^2, at a location on the centerline of the thruster at 5 cm downstream. Electron temperature and density measurements were also made using a triple Langmuir probe on centerline at 5 cm

downstream. Average measurements of peak electron temperature were about 1 eV and peak electron density of about 1.5×10^{11} cm^{-3}.

Ablation mass characterization yields an average mass bit of about 250 µg. Extending the plasma measurements to this value yields an ionization fraction of < 1% of the ablation mass. Comparing these results to traditional Teflon PPT performance characteristics show that the HIPEP microthruster has a lower ion current density, electron temperature, electron density and ionization fraction, but a mildly larger ablation mass bit. These results suggest that the microthruster exhibits an acceleration mechanism dominated by electrothermal energy, a property typical of PPT's, in a much more exaggerated form. More study is needed to confirm or deny this hypothesis.

Acknowledgments

References

[1]Sawka, W. N., A. Katzakian and C. Grix, "Solid State Digital Cluster Thrusters for Small Satellites, Using High Performance Electrically Controlled Extinguishable Solid Propellants," Paper SSC05-XI-3, 19th Annual AIAA/USU Small Satellite Conference, 2005.

[2]Grix, C; Katzakian, A.; Sawka, W.N.; "Throttled Propulsion Using and Electrically Controlled Extinguishable Solid Propellant Dual Stage Motor," 24th JANNAF Rocket Nozzle Technology Subcommittee Meeting, (*Invited*), San Diego, CA, November 2005

[3]Katzakian, A; Grix, C; and Sawka W.N.; "Electrically Controlled Extinguishable Solid Propellants: A Safe, Broadly Scalable Propulsion Technology," 53rd JANNAF Propulsion Mtg, Monterey, CA, December 2005

[4]Sawka, W. N., "Pulse Performance and Power Requirements for Electrically Controlled Solid Propellant," 54th JANNAF Propulsion Meeting, Denver, CO, May 14-17, 2007

[5]Sawka, W. N. and McPherson, M., "Electrical Solid Propellants: A Safe, Micro to Macro Propulsion Technology," 49th AIAA/ASME/SAE/ASEE Joint Propulsion Conference, San Jose, CA, July 2013

[6]Burton, R. L., and Turchi, P. J., "Pulsed Plasma Thruster", *Journal of Propulsion and Power*, Vol. 14, No. 5, 1998.

[7]Andrenucci, M., Lensi, R., Naso, V., and Melli, R., ''Design of Solid-Propellant MPD Thrusters,'' *Electric Propulsion and Its Application to Space Missions*, edited by R. C. Fincke, Vol. 79, Progress in Astronautics and Aeronautics, IAA, New York, 1980, pp. 586– 601.

[8]Guman, W. J., and Nathanson, D. M., ''Pulsed Plasma Microthruster Propulsion System for Synchronous Orbit Satellite,'' *Journal of Spacecraft and Rockets*, Vol. 7, No. 4, 1970, pp. 409– 415.

[9]Vondra, R. J., and Thomassen, K. I., ''Flight Qualified Pulsed Electric Thruster for Satellite Control,'' *Journal of Spacecraft and Rockets*, Vol. 11, No. 9, 1974, pp. 613– 617; also AIAA Paper 73-1067, Oct. 1973.

[10]Vondra, R. J., ''The MIT Lincoln Laboratory Pulsed Plasma Thruster—A Final Report on the LES-8/9 Pulsed Plasma Thruster,'' AIAA Paper 76-998, Nov. 1976.

[11]LaRocca, A. V., ''Pulsed Plasma Thruster System for Attitude and Station Control of Spacecraft,'' *First Western Space Congress*, 1970, pp. 688 – 702.

[12]Akimov, V., Nagel, I., Ogloblina, I., Antropov, N., Pokryshkin, A., Popov, G., and Rudikov, A., ''Analysis of PPT Potentialities in Solving the Satellite Orbit Control Tasks,'' 25th International Electric Propulsion Conf., Paper 97-146, Aug. 1997.

[13]Janson, S. W., "The On-Orbit Role of Electric Propulsion," AIAA Paper 93-2220, June 1993.

[14]Meckel, N. J., Cassady, R. J., Osborne, R. D., Hoskins, W. A., and Myers, R. M., ''Investigation of Pulsed Plasma Thrusters for Spacecraft Attitude Control,'' 25th International Electric Propulsion Conf., Paper 97-128, Aug. 1997.

[15]Cassady, R. J., Meckel, N. J., Hoskins, W. A., Myers, R. M., Oleson, S. R., and McGuire, M., ''Pulsed Plasma Thruster Systems for Spacecraft Attitude Control,'' 10th AIAA/Utah State University Conference on Small Satellites, Sept. 1996.

[16]US Patents 7,958,823 B2 June 14 2011, and 8,464,640 June 18 2013, "Controllable Digital Solid State Cluster Thrusters for Rocket Propulsion and Gas Generation"

[17]Vondra, R., Thomassen, K., and Solbes, A., "A Pulsed Electric Thruster for Satellite Control," *Proceedings of the IEEE*, Feb. 1971

[18]Rovey, J. L., Walker, M. L. R., Gallimore, A.D., and Peterson, P.Y., "Evaluation of a Magnetically-Filtered Faraday Probe for measuring the ion current density profile of a Hall thruster," 40th AIAA/ASME/SAE/ASEE Joint Propulsion Conference and Exhibit, July 2004.

[19]Eckman, R., Gatsonis, N.A., Myers, R. M., and Pencil, E. J., "Experimental Investigation of the LES 8/9 Pulsed Plasma Thruster Plume," International Electric Propulsion Conference, AIAA Paper IEPC-97-126, 1997

[20]Chen, F. F., "Lecture Notes on Langmuir Probe Diagnostics," Mini-Course on Plasma Diagnostics, IEEE-ICOPS meeting, Jeju, Korea, June 5, 2003.

[21]Eckman, R., "Pulsed Plasma Thruster Plume Diagnostics," 36th AIAA Aerospace Sciences Meeting and Exhibit, Paper 10.2514/6.1998-4, January, 1998.

[22]Eckman, R., Byrne, L., Gatsonis, N.A., and Pencil, E. J., "Triple Langmuir Probe Measurements in the Plume of a Pulsed Plasma Thruster," *Journal of Propulsion and Power*, 2001, Vol. 17, No. 4, pp. 762-771

[23]Byrne, L., Zwahlen, J., Gatsonis, N., and Pencil, E. J., "Pulsed Plasma Thruster Plume Measurements Using a Triple Langmuir Probe Method," 38th AIAA/ASME/SAE/ASEE/ Joint Propulsion Conference and Exhibit, Paper 10.2514/6.2002-4126, 2002.

[24]Walker, M. L. R., Hofer, R. R., Gallimore, A. D., "The Effects of a Nude Faraday Probe Design and Vacuum Facility Backpressure on the measured ion current density profile of Hall thruster Plumes," AIAA-2002-4253, 38th Joint Propulsion Conference, Indianapolis, IN, July 7-10, 2002.

[25]Chen, S. -L. and Sekiguchi, T., "Instantaneous Direct-Display System of Plasma Parameters by Means of Triple-Probe," *Journal of Applied Physics*, Vol. 36, No. 8, pp. 2363-2375, August 1965.

[26]Chen, S. -L., "Studies of the Effect on Ion Current on Instantaneous Triple-Probe Measurements," *Journal of Applied Physics,* Vol. 42, No. 1, 1971, pp. 406-412.

[27]Haag, T. W., "PPT Thrust Stand," AIAA Paper 95-2917, July 1995; also NASA TM 107066, July 1995.

[28]Sasoh, A., and Arakawa, Y., "A High-Resolution Thrust Stan for Ground Tests of Low-Thrust Space Propulsion Devices," *Review of Scientific Instruments*, Vol. 64, No. 3, 1993, pp. 719-723.

[29]Keidar, M., Boyd, I. D., Beilis, I. I., "Model of an Electrothermal Pulsed Plasma Thruster," *Journal of Propulsion and Power*, Vol. 19, No. 3, June 2003, pp. 424-430.

[30]Thomassen, K. I., and Vondra, R. J., "Exhaust Velocity Studies of a Solid Teflon Pulsed Plasma Thruster," *Journal of Spacecraft and Rockets*, Vol. 9, No. 1, 1972, pp. 61-64.

[31]Lau, M., Manna, S., Herdrich, G., Schönherr, T., Komurasaki, K., "Investigation of the Plasma Current Density of a Pulsed Plasma Thruster," *Journal of Propulsion and Power*, Vol. 30, No. 6, 2014, pp. 1459-1470.